Characterization of the Performance of a Custom Program for Image Processing of Pressure Sensitive Film

Muturi G. Muriuki[1]
Ph.D.
e-mail: mgmst20@pitt.edu

Lars G. Gilbertson
Ph.D.

Christopher D. Harner
M.D.

Department of Orthopaedic Surgery,
University of Pittsburgh,
Pittsburgh, PA 15261

A custom program for the processing of pressure sensitive (Fuji) film data is presented and validated in this paper. Some of the shortcomings of previous descriptions of similar programs in literature are addressed. These shortcomings include incomplete descriptions of scan resolution, processing technique, and accuracy of results. Of these, the accuracy of results is the most important and is addressed in this study by using Fuji film calibration data. In Fuji film calibration, known loads are applied to forms with known area. The accuracy of this program and that of the two commercially available image processing programs were determined. The results of the custom program are found to be within 10% of the results from the commercial programs and from experimental data. This level of accuracy is the same reported level of accuracy of Fuji film, verifying the custom program for use in Fuji film contact pressure and area measurements.
[DOI: 10.1115/1.3005150]

Keywords: Fuji film, resolution, accuracy, contact area, contact pressure, comparison, validation

Introduction

Fuji Pressensor or Prescale pressure sensitive film (Fuji Photo Film Co., Ltd., Tokyo, Japan) has been used to measure both contact pressure and area in a variety of applications. These applications, initially industrial in nature, have extended to a variety of purposes; including being used to measure joint contact pressures and areas [1–5].

Fuji Prescale film consists of two sheets. The A sheet has ink-filled microscopic bubbles that burst at different pressures over a particular range (the range is determined by Fuji film type). The C sheet has a developer that turns the ink released from the A layer red. As the applied pressure increases more bubbles burst, increasing the intensity of the red stain [6]. This property of Fuji film lends itself to optical measurement of stain intensity. Stain intensity can be converted to applied pressure using the manufacturer's optical comparison charts, which depend on a subjective evaluation that compares stain intensity to the intensities in the chart [7–11], optical densitometers [12–14], or, more commonly, by using experimentally determined calibration curves [15–31,4,5]. In addition, the spatial resolution of both the optical comparison charts and optical densitometers is limited by the subjective nature of the intensity conversion and the scan area of the densitometer. Various optical and nonoptical methods have been used for determining the area. The nonoptical methods estimate the contact area by measuring the area by hand from the film. The optical techniques digitize the image and use an analysis program to determine the area [32–34]. In some studies, image analysis was carried out on a scanned film using a commercially available software. The image processing and analysis techniques include thresholding and use of filters, but detail of the threshold level and type of filter used is rarely given. When stated, the resolution of the scanned images is rarely given a numerical value and is often described as "high." In turn, the accuracy of the pressure or area measurements is rarely addressed in these studies.

In this paper, a custom Fuji film processing program for determining the contact area and contact pressure is described. The custom program is verified by checking the results obtained against that from two commercially available software programs commonly used in Fuji film processing. The data used to test and verify the programs are from a series of Fuji film calibration experiments.

Fuji Film Calibration

Fuji film calibration was performed as follows. The two sheets of film were cut to size, put together, and placed between the base and punch. The crosshead of a material testing machine (TTS–25kN, Adelaide Testing Machines Inc., Toronto, ON, Canada) was then lowered until the stud in the load cell contacted the punch. Figure 1 shows the setup used to calibrate the Fuji film. The load was then increased, by further lowering the crosshead, to the particular load set point. Load and crosshead position data were recorded at 10 Hz. The portion of the punch in contact with the film has a diameter of 25.4 mm. Fuji film stains produced have the same area as the punch. Applied stress can be calculated from the load data. Stains were optically scanned at a spatial resolution of 600 dpi (HP Scanjet 5550c, Hewlett-Packard Company, Palo Alto, CA) and saved as 8 bit grayscale TIFF images. Applied pressure can be calculated from the punch area and applied load. The area of the punch was used to verify the area calculation of the image processing programs. The average pressures as determined by the image processing programs were compared against each other.

Description of the Custom Image Processing Program

Ten scanned Fuji films stains were chosen from calibration data (the first six were low Fuji film with a pressure range from 2.4 MPa to 9.7 MPa and the last four superlow Fuji films with a pressure range from 0.5 MPa to 2.4 MPa). The 8 bit grayscale images were loaded into the custom MATLAB program (The MathWorks Inc., Natick, MA) and converted to pressure images using a fifth order polynomial fit to the calibration data as described by Liggins et al. [2]. The correlation coefficients ($R2$) for the fifth order polynomial fit ranged from 0.96 to 0.98 (Fig. 2). The equation of the fifth order polynomial fit relates applied load (or pressure) to optical density. The ten pressures were evenly spread over the Fuji film range with points in the high and low pressure saturation regions.

After conversion and before performing calculations of contact area and contact pressure, pressure images were filtered with a 25×25 pixel averaging filter to remove noise (at 600 dpi this corresponds to approximately a 1×1 mm^2 filter). Noise in the image is assumed to cause variations in the value of individual pixels that is not correlated with the values of neighboring pixels. The averaging filter replaces each individual pixel value with the average value of the pixels in the surrounding 25×25 pixel area. The filter automatically adjusts the size of the filter to handle averages for pixels close to the image boundary, excluding pixels that fall outside the image boundary e.g., the filter will average

[1]Corresponding author.

Contributed by the Bioengineering Division of ASME for publication in the JOURNAL OF BIOMECHANICAL ENGINEERING. Manuscript received August 28, 2007; final manuscript received August 4, 2008; published online November 21, 2008. Review conducted by Avinash Patwardhan.

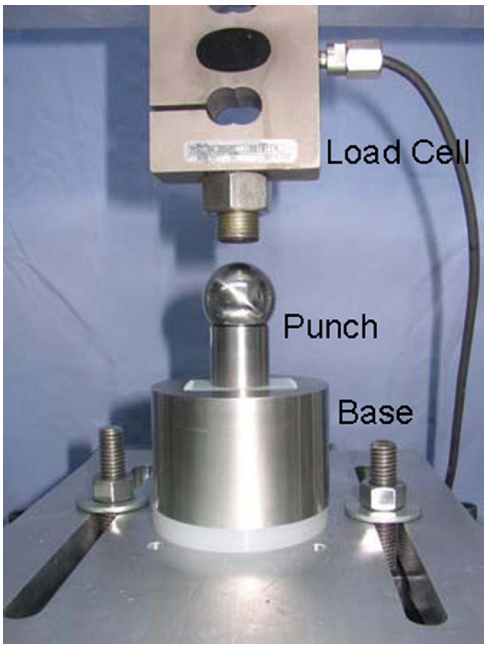

Fig. 1 Picture of calibration setup

values from a square with a 13 pixel side length for a pixel in the top left hand corner of the image. The size of the image is unchanged by the filter as a result of the adjustments in filter dimension at the boundaries.

Artifact introduced during preparation and handling of the Fuji film was excluded by introducing a threshold pressure value of 0.1 MPa. To calculate the area, all pixels in the pressure image with a pressure value above the threshold value were summed. This number was converted to area using the scan resolution. For the average pressure, the pixels with a pressure value greater than the threshold value of 0.1 MPa were averaged.

SCION IMAGE for Windows (Scion Corp., Frederick, MD) and METAMORPH (Molecular Devices Corp., Downington, PA) were the image processing programs chosen to compare against our custom program. 600 dpi scans from the ten Fuji film calibration stains were loaded into SCION and METAMORPH in turn. Thresholding was used to select regions of interest over which optical density was averaged. Threshold level was selected using a slider. The area selected by the threshold level chosen was displayed by way of a black and white image in the user interface. This average optical density was converted to pressure using the fifth order polynomial fit (Fig. 2). The region of interest was also used to determine the contact area. Contact area was not calculated using METAMORPH.

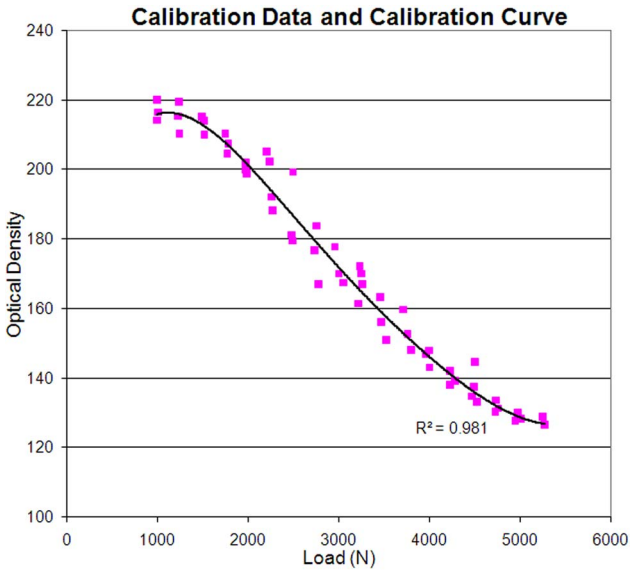

Fig. 2 Low Fuji film calibration data and calibration curve

Table 1 Calculated contact area

Test No.	MATLAB	SCION
1	507.9	535.5
2	518.5	548.4
3	516.5	541.9
4	524.6	541.9
5	368.2	554.8
6	465.9	541.9
7	524.2	535.5
8	528.5	541.9
9	514.6	535.5
10	507.1	548.4
Average (SD)	497.6 (48.8)	542.6 (6.5)

Results of Verification

The actual area of the face of the 25.4 mm diameter punch was 507 mm^2. As shown in Table 1 average contact areas calculated by MATLAB and SCION were 498 ± 49 mm^2 and 543 ± 6 mm^2, respectively. These values are approximately 2% lower and 7% higher than the real contact area.

The higher standard deviation obtained from the custom program is a consequence of the saturation effect of the Fuji film. Figure 3 illustrates the saturation effect. Test number 4 is at a higher applied pressure than test 5 (white, 255 or 2^8-1, is no measured pressure). Fuji film has both a high and a low saturation effect. At the high level, increasing the applied pressure does not increase the red intensity; and at the low level, applied pressure is not high enough to burst the ink bubbles, registering as zero applied pressure. A consequence of this is that until the upper saturation level is reached, the contact area appears to grow with applied pressure. This saturation effect is masked by the algorithm used to calculate area in SCION, which does not allow a selection of a numerical threshold value for calculation of area but uses a slider bar to generate a binary image that is used in the calculations. All attempts were made to have the slider in the same position for all the data analyzed and the result is that SCION provides only four different numerical values for area (Table 1).

The average contact pressures obtained from SCION and METAMORPH were normalized to the value obtained from MATLAB.

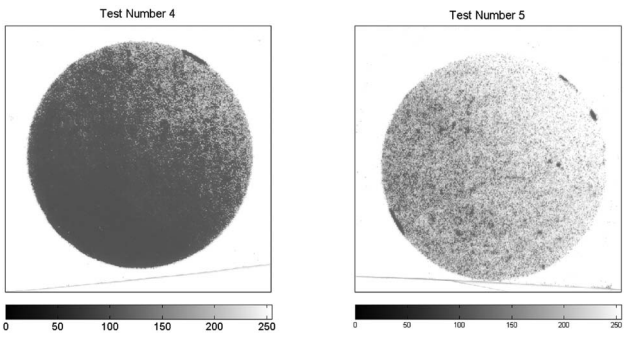

Fig. 3 8 bit grayscale scans from tests 4 and 5

Table 2 Calculated contact pressure

Test No.	Setpoint pressure (MPa)	MATLAB (MPa)	MATLAB/SCION	MATLAB/METAMORPH	
				No filter	Filtered
1	6.91	6.57	1.03	1.08	1.16
2	6.91	7.76	1.05	1.10	1.15
3	8.88	8.61	0.96	1.09	1.07
4	8.88	8.58	0.93	1.11	1.12
5	4.93	5.11	1.19	1.28	1.26
6	4.93	4.66	1.02	1.08	1.05
7	3.35	1.62	0.92	0.95	1.05
8	3.35	1.80	0.98	1.03	1.11
9	2.57	1.19	0.84	0.91	0.89
10	2.57	1.01	0.86	1.10	0.99
Average (SD)		—	0.98 (0.10)	1.07 (0.10)	1.09 (0.10)

In addition, a 25×25 pixel filter was implemented in METAMORPH to determine the effect of filtering on calculated pressure. As shown in Table 2 average contact pressure from MATLAB was 2% higher than from SCION, 7% lower than METAMORPH, and 9% lower than METAMORPH with the filter implemented.

All the calculated pressures and areas were within 10% of each other. Additionally, calculated area was within 10% of the experimental value. This level of accuracy is approximately that of the Fuji film, 10–15%, as reported in literature [35,2].

Conclusions

The custom MATLAB Fuji film image processing program presented calculates contact area and pressure values that are less than 10% different from area and pressure as calculated by commercially available image processing programs, and less than 10% different from the real contact area. This level of accuracy is the same as the accuracy reported in literature for Fuji film, validating the use of this custom program as developed and used in our laboratory for Fuji film image processing.

This custom program provides us with several benefits. We are able to process Fuji film without resorting to commercial image processing software. Additionally having written the custom program, the results are produced by known data transformations on our image data (e.g., the 25×25 pixel averaging filter, thresholding at 0.1 MPa) and not by black box operations (e.g., the filter function in METAMORPH). Further modules can also be easily programed to increase utility, functionality, and processing capability.

It is worth noting that the accuracy stated herein for the custom program is for hard surfaces. With this type of contact there is a relatively quick transition from high to zero pressure at the circumference of the punch. These edge effects affect the measurement accuracy. With softer biological materials there would be indentation and a slower pressure transition, which would affect the accuracy of pressure measurements with Fuji film. While 10% accuracy may not seem impressive, the actual accuracy of the image processing program may be masked by the accuracy of the Fuji film.

References

[1] Fukubayashi, T., and Kurosawa, H., 1980, "The Contact Area and Pressure Distribution Pattern of the Knee. A Study of Normal and Osteoarthrotic Knee Joints," Acta Orthop. Scand., **51**, pp. 871–879.

[2] Liggins, A. B., and Finlay, J. B., 1992, "Recording Contact Areas and Pressures in Joint Interfaces," *Proceedings of the International Conference on Experimental Mechanics: Technology Transfer Between High Tech Engineering and Biomechanics*, 1992, Limerick, Ireland, Elsevier Science Publishers, B.V.

[3] McGinley, J. C., Hopgood, B. C., Gaughan, J. P., Sadeghipour, K., and Kozin, S. H., 2003, "Forearm and Elbow Injury: the Influenceof Rotational Position," J. Bone Jt. Surg., Am. Vol. **85A**, pp. 2403–2409.

[4] Wang, C. L., Cheng, C. K., Chen, C. W., Lu, C. M., Hang, Y. S., and Liu, T. K., 1995, "Contact Areas and Pressure Distributions in the Subtalar Joint," J. Biomech., **28**, pp. 269–279.

[5] Wolchok, J. C., Hull, M. L., and Howell, S. M., 1998, "The Effect of Intersegmental Knee Moments on Patellofemoral Contact Mechanics in Cycling," J. Biomech., **31**, pp. 677–683.

[6] Singerman, R. J., Pederson, D. R., and Brown, T. D., 1987, "Quantitation of Pressure Sensitive Film Using Digital Image Scanning," Exp. Mech., **27**, pp. 99–105.

[7] Chen, M. I., Branch, T. P., and Hutton, W. C., 1996, "Is It Important to Secure the Horns During Lateral Meniscal Transplantation?, A Cadaveric Study," Arthroscopy: J. Relat. Surg., **12**, pp. 174–181.

[8] Heino Brechter, J., Powers, C. M., Terk, M. R., Ward, S. R., and Lee, T. Q., 2003, "Quantification of Patellofemoral Joint Contact Area Using Magnetic Resonance Imaging," Magn. Reson. Imaging, **21**, pp. 955–959.

[9] Lee, S. B., Itoi, E., O'Driscoll, S. W., and An, K. N., 2001, "Contact Geometry at the Undersurface of the Acromion With and Without a Rotator Cuff Tear," Arthroscopy: J. Relat. Surg., **17**, pp. 365–372.

[10] Moed, B. R., Ede, D. E., and Brown, T. D., 2002, "Fractures of the Olecranon: An In Vitro Study of Elbow Joint Stresses After Tension-Band Wire Fixation Versus Proximal Fracture Fragment Excision," J. Trauma: Inj., Infect., Crit. Care, **53**, pp. 1088–1093.

[11] Park, M. C., Cadet, E. R., Levine, W. N., Bigliani, L. U., and Ahmad, C. S., 2005, "Tendon-to-Bone Pressure Distributions at a Repaired Rotator Cuff Footprint Using Transosseous Suture And Suture Anchor Fixation Techniques," Am. J. Sports Med., **33**, pp. 1154–1159.

[12] Brown, T. D., Rudert, M. J., and Grosland, N. M., 2004, "New Methods for Assessing Cartilage Contact Stress After Articular Fracture," Clin. Orthop. Relat. Res., **423**(6), pp. 52–58.

[13] Deguchi, K., Takeuchi, N., and Shimizu, A., 2002, "Evaluation of Press-Uniformity Using a Pressure Sensitive Film and Calculation of Wafer Distortions Caused by Mold Press in Imprint Lithography," Jpn. J. Appl. Phys., Part 1, **41**(1), No. 6B (Special Issue: Microprocesses and Nanotechnology), pp. 4178–4181.

[14] Kuroda, R., Kambic, H., Valdevit, A., and Andrish, J. T., 2001, "Articular Cartilage Contact Pressure After Tibial Tuberosity Transfer. A Cadaveric Study," Am. J. Sports Med., **29**, pp. 403–409.

[15] Alhalki, M. M., Howell, S. M., and Hull, M. L., 1999, "How Three Methods for Fixing a Medial Meniscal Autograft Affect Tibial Contact Mechanics," Am. J. Sports Med., **27**, pp. 320–328.

[16] Atkinson, P. J., Newberry, W. N., Atkinson, T. S., and Haut, R. C, 1998, "Method to Increase the Sensitive Range of Pressure Sensitive Film," J. Biomech., **31**, pp. 855–859.

[17] Borrelli, J. Jr., Burns, M. E., Ricci, W. M., and Silva, M. J., 2002, "A Method for Delivering Variable Impact Stresses to the Articular Cartilage of Rabbit Knees," J. Orthop. Trauma, **16**, pp. 182–188.

[18] Cheng, C. K., Huang, C. H., Liau, J. J., and Huang, C. H., 2003, "The Influence of Surgical Malalignment on the Contact Pressures of Fixed and Mobile Bearing Knee Prostheses—a Biomechanical Study," Clin. Biomech. (Bristol, Avon), **18**, pp. 231–236.

[19] Diab, M., Poston, J. M., Huber, P., and Tencer, A. F., 2005, "The Biomechanical Effect of Radial Shortening on the Radiocapitellar Articulation," J. Bone Joint Surg. Br., **87**, pp. 879–883.

[20] Goh, J. C., Lee, P. Y., and Bose, K., 1995, "A Cadaver Study of the Function of the Oblique Part of Vastus Medialis," J. Bone Joint Surg. Br., **77**, pp. 225–231.

[21] Harris, M. L., Morberg, P., Bruce, W. J., and Walsh, W. R., 1999, "An Improved Method for Measuring Tibiofemoral Contact Areas in Total Knee Arthroplasty: A Comparison of K-Scan Sensor and Fuji Film," J. Biomech., **32**, pp. 951–958.

[22] Hsieh, Y. F., Draganich, L. F., Ho, S. H., and Reider, B., 2002, "The Effects of Removal and Reconstruction of the Anterior Cruciate Ligament on the Contact Characteristics of the Patellofemoral Joint," Am. J. Sports Med., **30**, pp. 121–127.

[23] Kim, S. J., Shin, J. W., Lee, C. H., Shin, H. J., Kim, S. H., Jeong, J. H., and Lee, J. W., 2005, "Biomechanical Comparisons of Three Different Tibial Tunnel Directions in Posterior Cruciate Ligament Reconstruction," Arthroscopy: J. Relat. Surg., **21**, pp. 286–293.

[24] Kuno, H., Nambu, M., Yoshimura, T., Ando, T., Saito, I., Nakajima, K., and Tamura, T. A., 2000, "A Practical Application of Pressure-Sensitive Film for Preventing Pressure Sores," Proceedings of the 22nd Annual International Conference of the IEEE Engineering in Medicine and Biology Society, 2000, Chicago, IL.

[25] Lakin, R. C., DeGnore, L. T., and Pienkowski, D., 2001, "Contact Mechanics of Normal Tarsometatarsal Joints," J. Bone Jt. Surg., **83-A**, pp. 520–528.

[26] Levine, R. G., Renard, R., Behrens, F. F., and Tornetta, P., 2002, "Biomechanical Consequences of Secondary Congruence After Both-Column Acetabular Fracture," J. Orthop. Trauma, **16**(2), pp. 87–91.

[27] Rajaai, S. M., Walsh, W. R., and Schindhelm, K., 1996, "Cadaver Studies to Obtain Articular Pressure in the Distal Radioulnar Joint Using Fuji Prescale Pressure Sensitive Film," Proceedings of the 18th Annual International Conference of the IEEE Engineering in Medicine and Biology Society, Bridging Disciplines for Biomedicine, 1996, Amsterdam, Netherlands.

[28] Rosenbaum, D., Eils, E., and Hillmann, A., 2003, "Changes in Talocrural Joint Contact Stress Characteristics After Simulated Rotationplasty," J. Biomech., **36**, pp. 81–86.

[29] Sekaran, S. V., Hull, M. L., and Howell, S. M., 1998, "Nonanatomic Location

of the Posterior Horn of a Medial Meniscal Autograft Implanted in a Cadaveric Knee Adversely Affects the Pressure Distribution on the Tibial Plateau," Am. J. Sports Med., **30**, pp. 74–82.
[30] Sparks, D. R., Beason, D. P., Eberhardt, A. W., and Bandak, F. A., 2002, "Contact Pressure Measurements in the Hip Joint: Effects of Femoral Angle in Greater Trochanter Loading," Proceedings of the 24th Annual Conference and the Annual Fall Meeting of the Biomedical Engineering Society, 2002.
[31] Tuoheti, Y., Itoi, E., Yamamoto, N., Seki, N., Abe, H., Minagawa, H., Okada, K., and Shimada, Y., 2005, "Contact Area, Contact Pressure, and Pressure Patterns of the Tendon-Bone Interface After Rotator Cuff Repair," Am. J. Sports Med., **33**, pp. 1869–1874.
[32] Baratz, M. E., Fu, F. H., and Mengato, R., 1986, "Meniscal Tears: The Effect of Meniscectomy and of Repair on Intraarticular Contact Areas and Stress in the Human Knee., A Preliminary Report," Am. J. Sports Med., **14**, pp. 270–275.
[33] McKellop, H. A., Sigholm, G., Redfern, F. C., Doyle, B., Sarmiento, A., and Luck, J. V. Sr., 1991, "The Effect of Simulated Fracture-Angulations of the Tibia on Cartilage Pressuresin the Knee Joint," J. Bone Jt. Surg., Am. Vol., **73**, pp. 1382–1391.
[34] Paletta, G. A. Jr., Manning, T., Snell, E., Parker, R., and Bergfeld, J., 1997, "The Effect of Allograft Meniscal Replacement on Intraarticular Contact Area and Pressures in the Human Knee. A Biomechanical Study," Am. J. Sports Med., **25**, 692–698.
[35] Hale, J. E., and Brown, T. D., 1992, "Contact Stress Gradient Detection Limits of Pressensor Film," ASME J. Biomech. Eng., **114**, pp. 352–357.